NATIONAL AERONAUTICS AND SPACE ADMINISTRATION

Technical Report 32-1397

The Hydraulic Characteristics of Flow Through Miniature Slot Orifices

Robert W. Riebling
Walter B. Powell

JET PROPULSION LABORATORY
CALIFORNIA INSTITUTE OF TECHNOLOGY
PASADENA, CALIFORNIA

September 15, 1969

NATIONAL AERONAUTICS AND SPACE ADMINISTRATION

Technical Report 32-1397

The Hydraulic Characteristics of Flow Through Miniature Slot Orifices

Robert W. Riebling
Walter B. Powell

JET PROPULSION LABORATORY
CALIFORNIA INSTITUTE OF TECHNOLOGY
PASADENA, CALIFORNIA

September 15, 1969

Prepared Under Contract No. NAS 7-100
National Aeronautics and Space Administration

Preface

The work described in this report was performed by the Propulsion Division of the Jet Propulsion Laboratory.

Acknowledgment

The authors wish to acknowledge the contributions of Jerry M. Newby and Donald R. Maxeiner, who carried out the flow experiments and the high-speed photography, respectively, and to thank Duane F. Dipprey for his many thoughtful suggestions and comments during the writing of this report.

Contents

Contents (contd)

Figures

Abstract

The hydraulic characteristics of miniature slot orifices of relatively short length and high aspect (width-to-height) ratio were studied experimentally. The effects of orifice dimensions, surface finish, and flow rates on discharge coefficients and flow regimes were determined. In addition, the stability and visual characteristics of the effluent liquid streams were observed. Orifice surface finish and length-to-height ratio were found to exert a primary influence on hydraulic behavior, and the flow from these devices was predominantly within the transition region. The results are directly applicable to the design of rocket engine injectors incorporating this type of orifice.

The Hydraulic Characteristics of Flow Through Miniature Slot Orifices

I. Introduction

In recent years, several variations of a novel liquid-propellant injection technique have been introduced to the rocket community. This technique makes use of a great many slot-like injection orifices, each with a flow area on the order of 10^{-4} to 10^{-5} in.^{2}, arranged in close proximity across the face of the injector. (One common arrangement is shown in Fig. 1.) The advantages of using a large number of very small orifices have long been recognized; these include: (1) high combustion efficiencies as a result of improved atomization and more intimate propellant mixing, and (2) ease of injector-face cooling because of the transpiration effect. However, the implementation of such concepts had to await the advent of modern fabrication techniques, which made possible the rapid and economical manufacture of these devices on a production basis, while guaranteeing reproducible dimensions and surface finishes.

"Micro-orifice" injectors, as they will be termed in this report, are manufactured commercially by a number of different methods, some of which are proprietary. However, most of the techniques involve the layup into stacks (Refs. 1 and 2), or the rollup into a tight coil (Ref. 3) of thin metallic plates or ribbons into which slot-like flow passages have been formed by chemical milling, stamping, punching, or etching. The resulting orifices are usually rectangular in cross section and have aspect

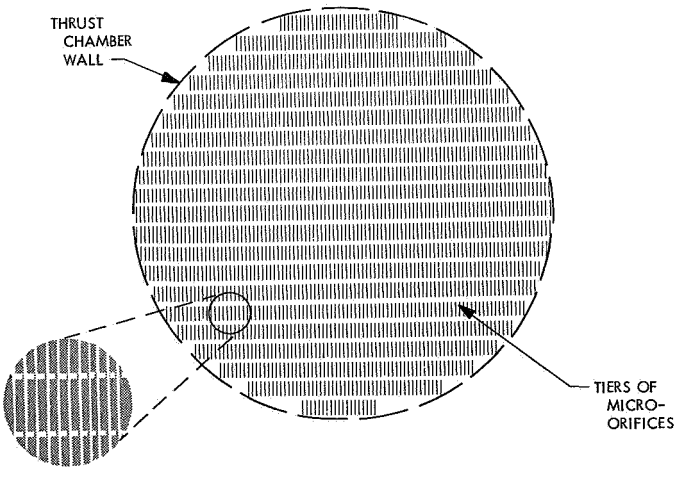

Fig. 1. Face of typical micro-orifice injector showing numerous slot orifices (artist's conception)

ratios (ratios of slot width w to height t) of 10 or more. In practice, the length-to-height L/t ratios of the slots seldom exceed 1000, and most often range between 50 and 100. The magnitude of the critical dimensions (0.001 in. $\lessapprox$ t $\lessapprox$ 0.003 in., and 0.030 in. $\lessapprox w \lessapprox$ 0.100 in.) of typical examples of these holes justifies use of the term, *micro*-orifice.

The use of these small, slot-like orifices in liquid-propellant rocket engine injectors presumes some understanding of their basic hydraulic characteristics. Metering the flow of propellants into a thrust chamber requires some knowledge of discharge coefficients, and how they are influenced by flow conditions, orifice geometry, and surface conditions. If the streams emerging from the slots are to impinge or otherwise interact, at least the rudiments of their geometry and stability must be understood. And in throttling applications, the flow regime (laminar, turbulent, or transitional) is of importance because of its influence on the relationship of pressure drop to flow rate.

Unfortunately, however, the requisite information is not to be found in the literature. The classical work with rectangular cross sections, both theoretical and experimental, has been concentrated on infinitely long ducts where fully developed velocity profiles prevail (e.g., Refs. 4, 5, and 6), and on flow areas of low aspect ratio ($w/t \lessapprox 10$). The injector micro-orifices, on the other hand, have low enough L/t ratios that fully developed flow may not, in general, be expected. Furthermore, because of their relatively high aspect ratios, the flow through such orifices is quite similar to that between infinitely wide parallel plates, where the aspect ratio per se ceases to be a significant variable. Discussions with cognizant representatives of the commercial manufacturers of these devices revealed a similar lack of all but the most cursory information on the hydraulic characteristics of rectangular micro-orifices.

Because of the increasing importance of micro-orifice injectors in present-day liquid-rocket technology, and because of other potential, injector-oriented applications of small, slot-like holes, a study of their gross hydraulic characteristics was undertaken at the Jet Propulsion Laboratory. The objective of this study was to determine the effects of geometry (dimensions and surface finish) and flow variables on the discharge coefficients and flow regimes of micro-orifices, as well as on the visual characteristics of the liquid streams emerging from them.

The study was by no means all-inclusive, and many aspects of this type of flow remain to be investigated. However, the key variables have been identified and the parametric variations of interest to the rocket injector designer have been developed. This report presents the results of that investigation.

II. Apparatus

The configuration of a typical slot-flow device is represented schematically in Fig. 2. For clarity, some dimensions have been exaggerated, and some details, such as fasteners and pipe fittings, have been omitted. The apparatus consisted of a stainless steel orifice block with a rectangular channel of length L, width w, and height t machined into its upper surface. This channel led from an internal manifold cavity, the dimensions of which were very large compared to those of the channel, to the exterior of the block. When the stainless steel cover plate was fastened securely to the orifice block, its highly polished lower surface S3 formed the fourth boundary side of the rectangular duct and the upper side of the manifold cavity. The use of a large fluid entrance port in conjunction with this voluminous cavity helped provide nearly stagnant conditions upstream of the orifice. The pressure tap was so located as to permit the measurement of fluid static pressure immediately ahead of the orifice entrance.

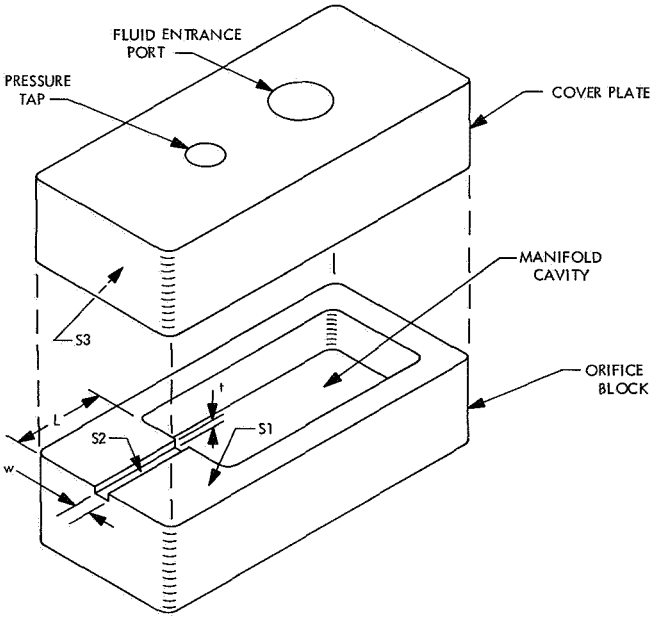

Fig. 2. Schematic representation of typical slot flow device

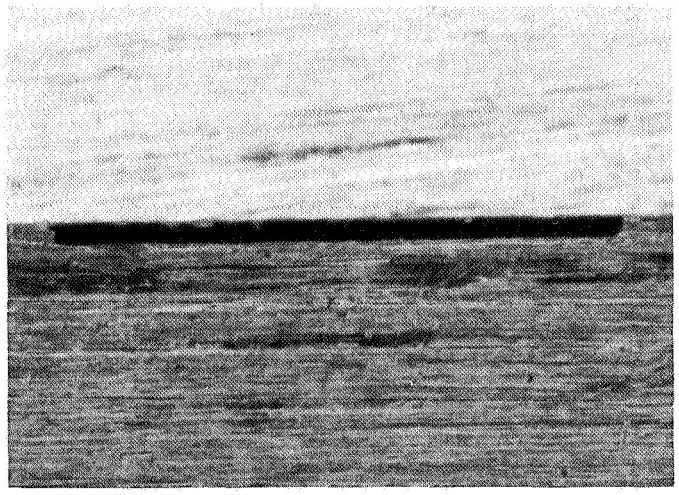

Fig. 3. End view of 0.003 × 0.100-in. slot

Orifice blocks with channel lengths L of nominally 0.05, 0.10, 0.20, and 1.0 in. were fabricated. Originally, these all had slot heights t of about 0.003 in. In the course of study, the t-dimension of each was progressively reduced to about 0.001 in. by grinding down the upper surface S1 of the orifice block. The width w remained constant at approximately 0.100 in. throughout the program. Figure 3 shows an end view of one of the slots formed by assembling the cover plate and orifice block, and Fig. 4 illustrates the four slot lengths employed.

The surface finish indicated in the photomacrographs (Fig. 4) was produced by grinding, and was typically ± 5 μin. rms parallel to the striations and 13 μin. perpendicular to them. This finish was characteristic of the lower surface S3 of the cover plate, which formed one side of the flow passage, and its mating surface S1.

In most instances, the lower surface S2 of the flow passage was also formed by grinding, and had the same characteristic surface finish (Fig. 5a). However, in a limited number of cases other techniques were used to form the surface S2. These included hand-honing the ground surface (Fig. 5b), electric-discharge machining (Fig. 5c), and hand-honing the electric-discharge-machined surface (Fig. 5d). Honing was found to exert a considerably greater influence on the electric-discharge-machined surfaces than on the ground surfaces. It should be noted that the electric-discharge-machined surfaces are quite similar to those produced by chemical-milling (acidic ferric chloride) in a typical, commercially produced* micro-orifice injector (Fig. 6), which justifies their inclusion in this study. Both processes remove small parcels or "domains" of material from the surface, leaving a characteristic dimpled appearance.

It should be kept in mind that the honed or electric-discharge-machined surfaces formed only one side of each slot. In all cases, the other side was the 5-μin. ground surface of the cover plate.

III. Experimental Procedures

After each machining modification, the dimensions and surface finishes of the individual orifices were measured by the JPL Inspection Department, and the actual, rather than the nominal, dimensions were used in calculating flow parameters such as the Reynolds number Re.

Each test device was mounted in the JPL spray-test facility and flowed vertically downward into ambient air. The test fluids were distilled water, trichlorethylene, and commercial grade n-hexane. Steady-state flow rates were determined by the timed collection of effluent in precision volumetric apparatus. Fluid temperature was measured for each data point so that the proper liquid density could be used in converting the flows to a gravimetric basis. Static pressure was measured to within $\pm 2\%$ using precision Bourdon gages.

During selected experiments, high-speed microflash still photographs were made to document the visual appearance of the emerging liquid streams, and high-speed (7000 frames/s), stroboscopically illuminated motion pictures were taken to assess their stability.

IV. Results and Discussion

This section defines terms used in the report, describes the effects of various parameters on discharge coefficient c_d and flow regime, and discusses the phenomenon of "hydraulic flip," characteristics of streams from slot orifices, and limitations on slot depth.

A. Definition of Terms

1. Orifice discharge coefficient. In the turbulent flow of fluids through orifices, a parameter known as a discharge coefficient c_d has been found to be quite useful in representing the degree of energy loss sustained by the stream upon discharge. One way of defining this coefficient is

$$c_d \equiv \frac{\dot{w}}{A(2g_c\rho\Delta p)^{1/2}} \equiv \left(\frac{\rho\bar{V}^2}{2g_c\Delta p}\right)^{1/2} \quad (1)$$

*HIPERTHIN injectors, a product of Aerojet-General Corp., Sacramento, Calif.

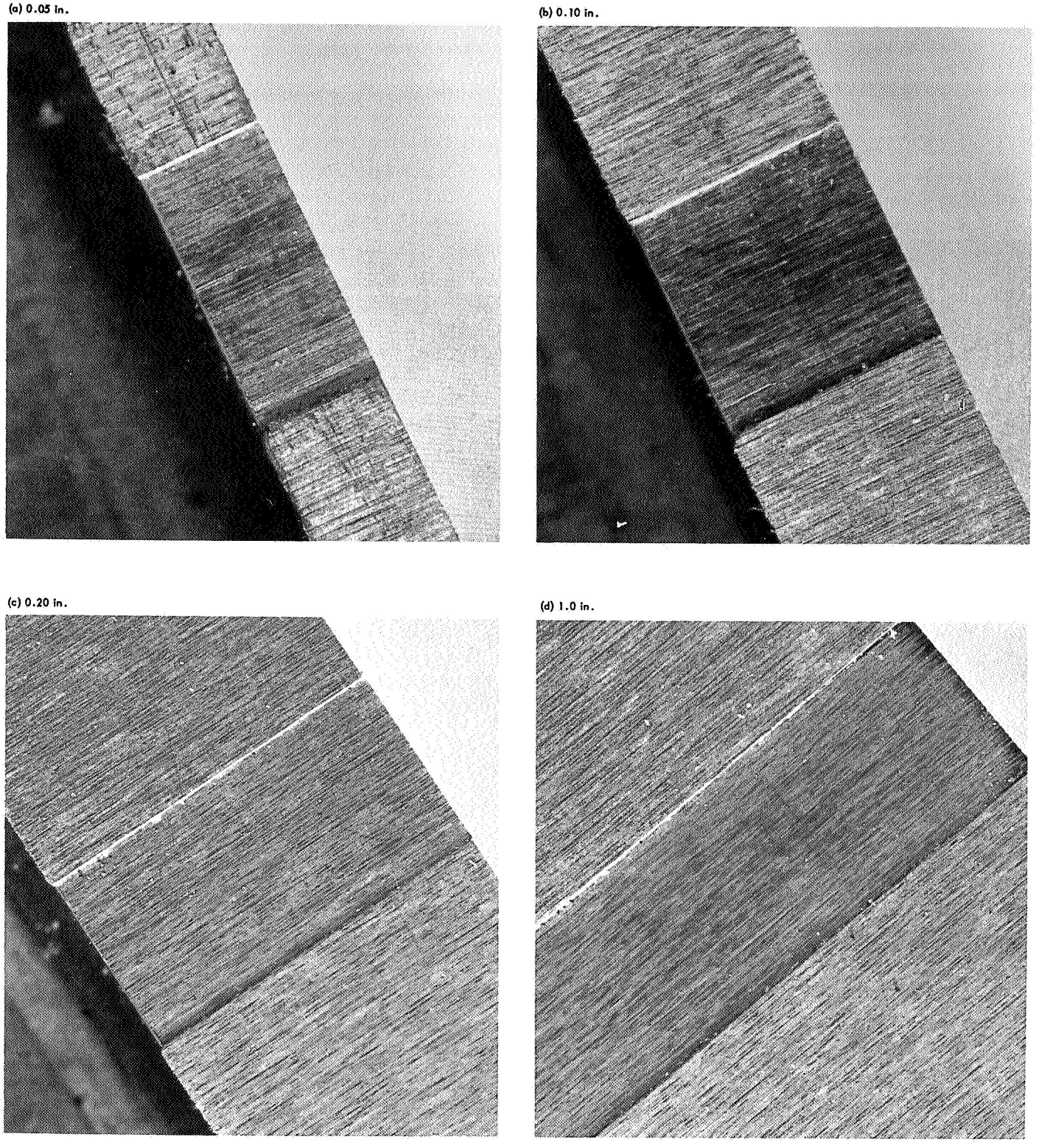

Fig. 4. Typical slot lengths investigated (shown for 0.002 × 0.100-in. slots with 5-μin. surface finish)

(a) GROUND—5 μin. rms PARALLEL TO FLOW

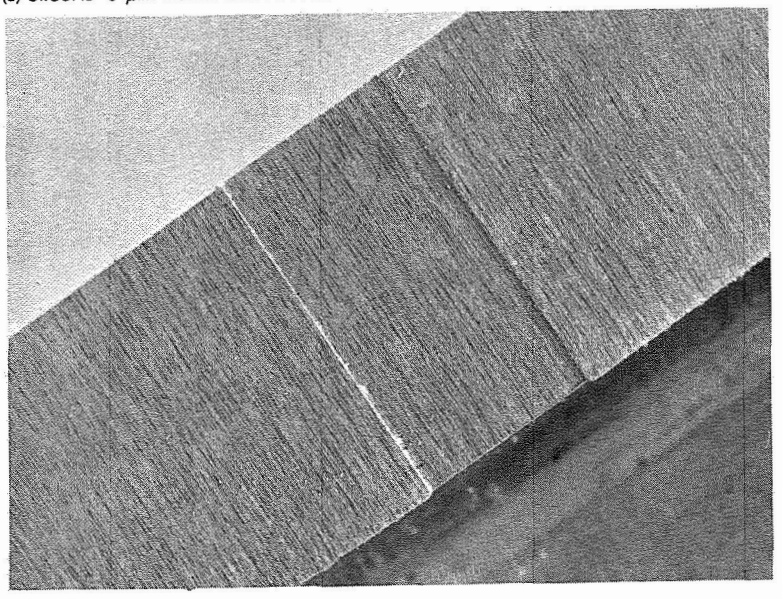

(b) GROUND AND HONED—4 μin. rms PARALLEL TO FLOW

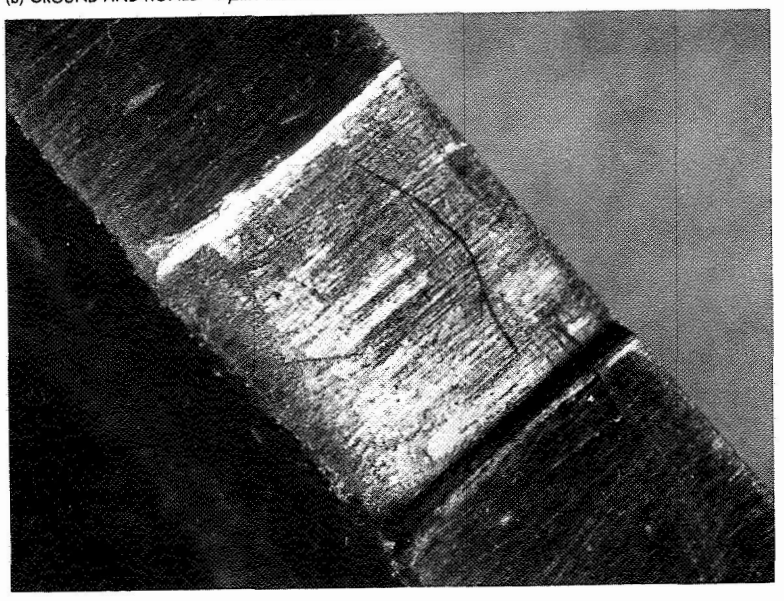

(c) ELECTRIC-DISCHARGE MACHINED—30 μin. rms PARALLEL TO FLOW

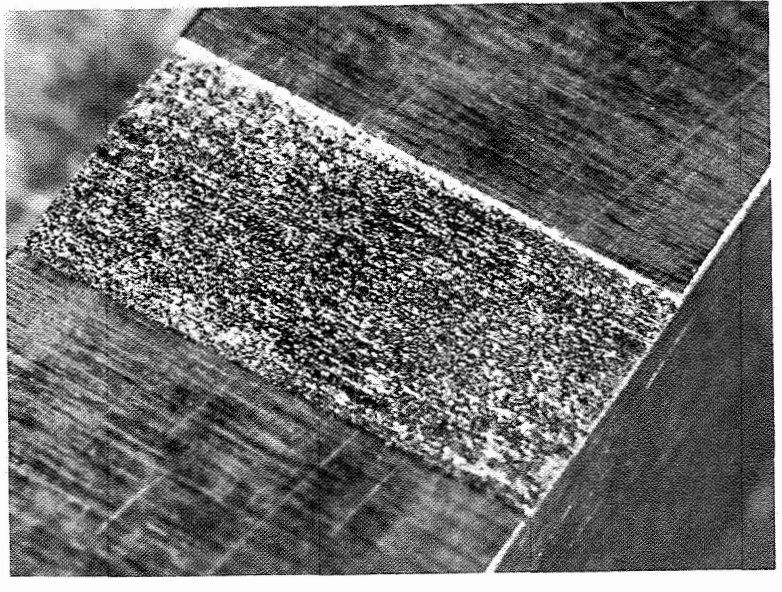

(d) ELECTRIC-DISCHARGE MACHINED AND HONED—30 μin. rms PARALLEL TO FLOW

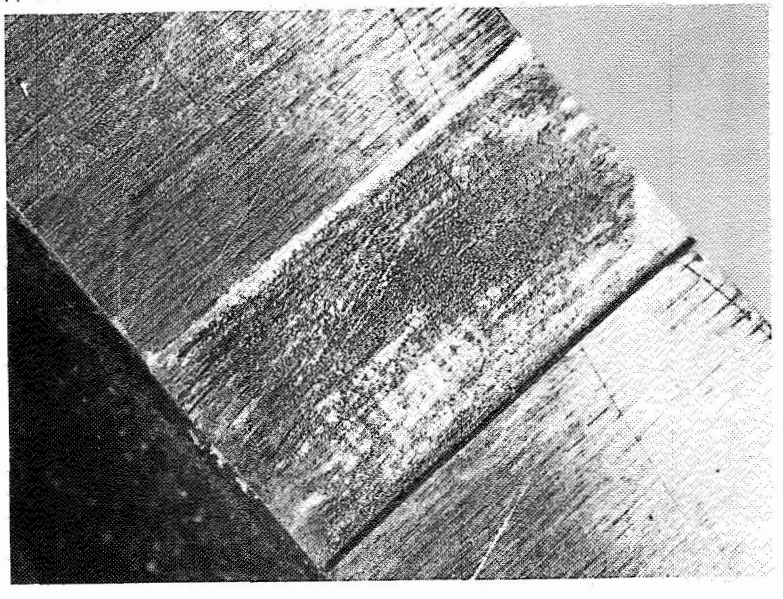

Fig. 5. Appearance of various slot surfaces investigated (shown for 0.003 × 0.100-in. slots)

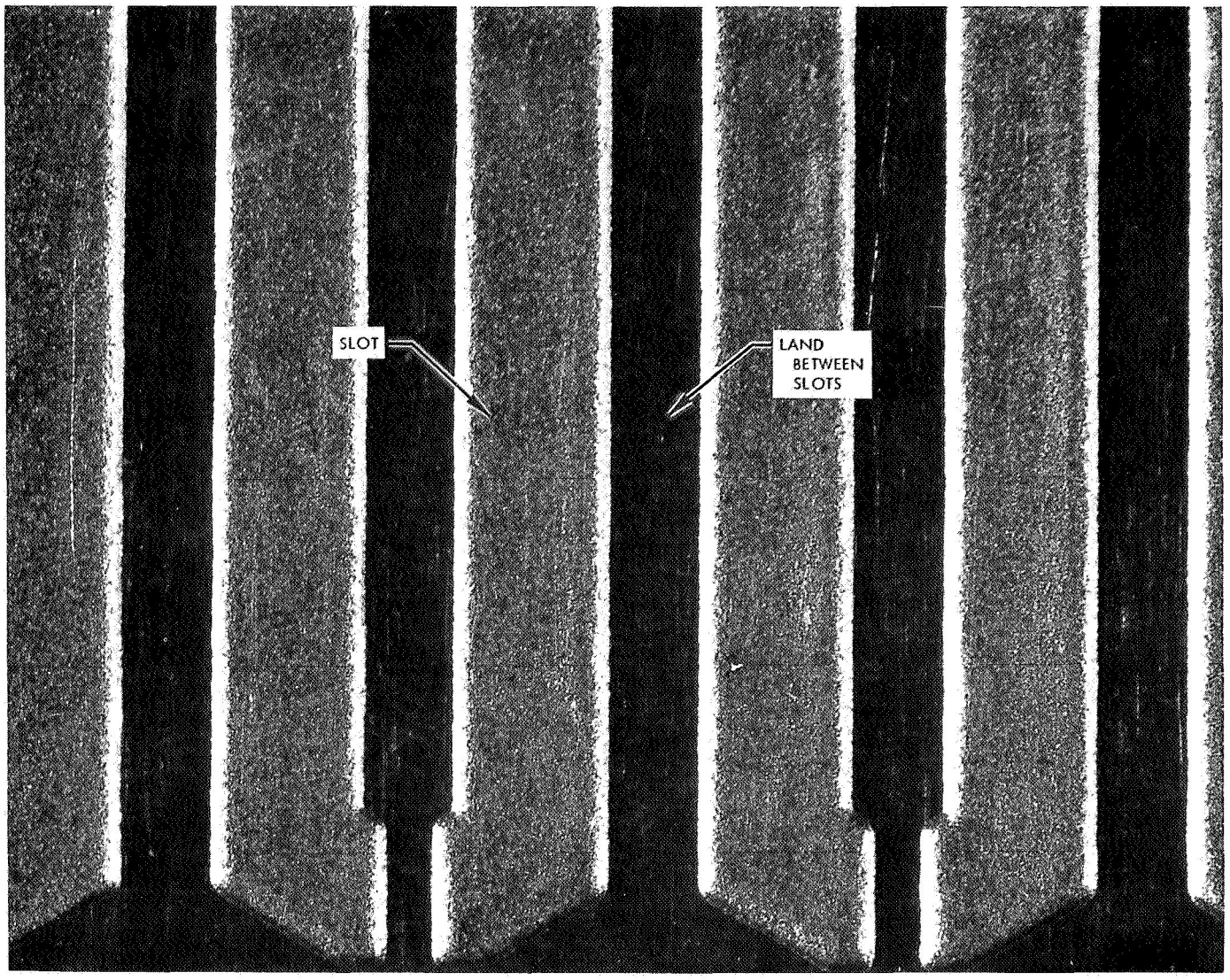

Fig. 6. Appearance of chemically milled slots from commercially produced injector (20 μin. rms parallel to flow)

in consistent units. As demonstrated in the Appendix, c_d may be further broken down as follows:

$$c_d \equiv \left(\frac{1}{c_c^2 c_v^2} + 2K_v - \frac{2}{c_c c_v} + \frac{2fL}{t} \right)^{-1/2} \qquad (2)$$

where c_c and c_v are contraction and velocity coefficients, K_v is a velocity-head coefficient, and f is the Fanning friction factor; $K_v = 1$ for turbulent flow and 1.6 for laminar flow, c_c is a function of Reynolds number and entrance geometry for turbulent flow and of entrance geometry only in laminar flow, and f is a function of Reynolds number and the duct wall roughness in turbulent flow and of Reynolds number only in laminar flow. One would expect, then, that c_d itself would be a function of Reynolds number, geometry, and wall roughness, and it is correlated in terms of those parameters in this report. The detailed determination of the individual terms in Eq. (2) was deemed to be beyond the scope of this rather limited investigation, although they are considered in the discussions of the results. The measurement and correlation of friction factors and entrance loss coefficients would, however, be a logical extension to the present work.

The parameter c_d will be used throughout this report to provide a convenient figure of merit with which to rate the relative efficiency of discharge without tacitly introducing ungrounded assumptions with regard to the

various terms in Eq. (2). It expresses the relationship between the experimentally measured values of mass flow rate and pressure drop.

2. Flow Reynolds number. The Reynolds number is the dimensionless ratio of inertial to viscous forces. In treating the flow through noncircular cross sections, it is customarily defined in terms of a "hydraulic diameter" D_h:

$$Re \equiv \frac{D_h \bar{V} \rho}{\mu} \tag{3}$$

where $\bar{V} \equiv \frac{\dot{w}}{\rho A}$

The hydraulic diameter is defined as:

$$D_h \equiv \frac{wt}{w + t} \tag{4}$$

However, with high-aspect-ratio slots, such as those employed in the present study, $w \gg t$, so that

$$D_h \cong t \tag{5}$$

and

$$Re \cong \frac{t \bar{V} \rho}{\mu} \tag{6}$$

Eq. (6) is the definition of Reynolds number used in this report.

3. Weber number. The Weber number We is the dimensionless ratio of inertial to surface forces. It is defined as

$$We \equiv \bar{V} t^{1/2} \left(\frac{\rho}{\sigma g_c} \right)^{1/2} \tag{7}$$

where t is taken to be the significant length dimension.

B. Effect of Surface Finish on Discharge Coefficient

The effect of three of the surface finishes shown in Fig. 5 on the discharge coefficient c_d at constant geometry is illustrated in Fig. 7. It is seen that at any particular value of the Reynolds number the ground surface with a roughness of 5 μin. rms parallel to the direction of flow exhibits the highest value of c_d. That is, for a given differential pressure across the length of the orifice, the one with the ground surface will pass the most mass. The unmodified 50-μin. electric-discharge-machined surface gave the lowest value of c_d, but this was significantly improved by honing. These effects must be considered to be relative only, since one side of the passage was formed by the ground surface of the cover plate.

It may be predicted that a device with the same geometry but having a 20-μin. chemically milled surface similar to that of Fig. 6 on one side would produce a curve intermediate to those of the ground and the honed electric-discharge-machined surfaces in Fig. 7. (Note that the curve for the plain electric-discharge-machined surface levels out at a much lower Reynolds number than the others.) Such a leveling is usually associated with the attainment of "fully-rough" flow, and it is not surprising that such a rough surface should induce the transition to Reynolds number-independent flow at lower values of Re. Based on these results, all subsequent work was carried out using only the ground surfaces.

C. Effect of Orifice Entrance Geometry on Discharge Coefficient

The effect of sharp vs rounded entries on the discharge coefficient at constant geometry is shown in Fig. 8. Although one surface was ground only, whereas the other was ground and then honed, their surface finishes were virtually identical; the significant effect shown in Fig. 8 is that of the entrance conditions. It is observed that rounding the entrance (putting an 0.020-in. radius on the upstream end of surface S2 in Fig. 2) markedly increased c_d at any fixed value of Re. Additionally, comparison of the lower curve of Fig. 8 with the upper curve of Fig. 7 gives an indication of the influence of orifice length on c_d, entrance and surface conditions being the same. At a Reynolds number of 2000, increasing L/t from 33 (Fig. 8) to 67 (Fig. 7) reduces c_d from 0.67 to 0.59 because of the additional fluid friction. All subsequent work was conducted with orifices having ground surfaces and rounded (0.015- to 0.020-in. radius) entries.

Also plotted in Fig. 8 is a curve calculated from Eq. (2), assuming $c_c c_v \cong 1.0$ because of the rounded entrance, $K_v = 1.0$ for turbulent flow, and using values of the friction factor f found from the smooth-tube pipe-flow charts at equivalent Reynolds numbers. The effective value of L/t for the slot with the 4-μin. ground, honed surface was employed in the calculations. Good agreement between the calculated curve and the experimental data for the 4-μin. slot is seen in the turbulent regime ($Re > 2800$) where $K_v = 1$, indicating that surfaces with a finish of 4 μin. or smoother behave very

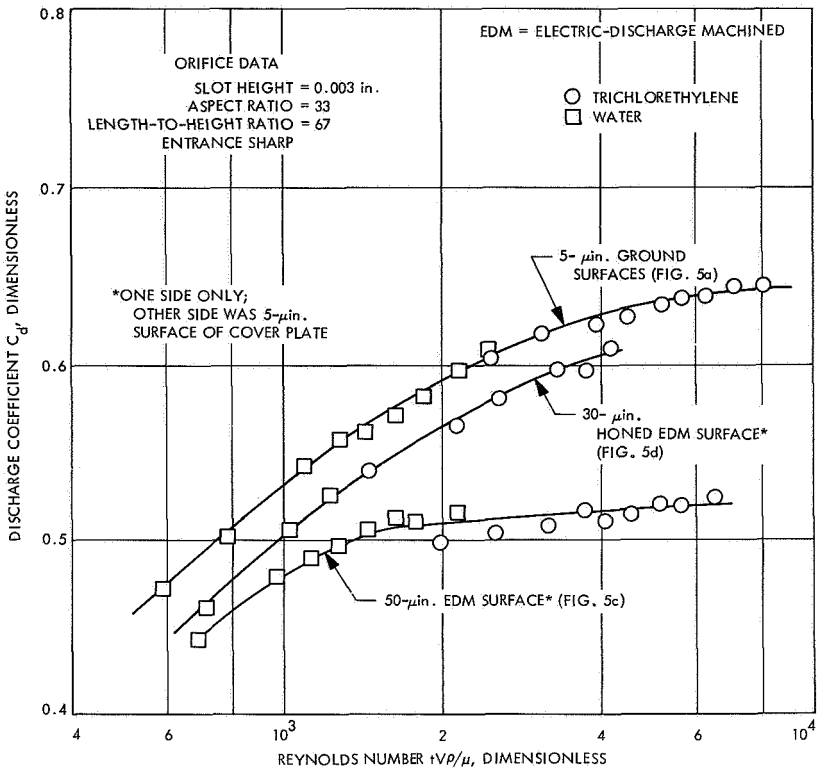

Fig. 7. Effect of surface finish on discharge coefficient at fixed geometry

much like completely smooth surfaces. Little would be gained, therefore, by attempting to manufacture slots with surface roughnesses less than 4 or 5 μin. rms.

Conversely, Eq. (2) may be applied to the top curve of Fig. 8 to obtain estimated values of f for 4-μin. ground and honed surfaces. Again assuming $c_c c_v$ and $K_v = 1$, $f = 0.0138$ at $Re = 2000$, and $f = 0.00682$ at $Re = 7000$. Using this information, the lower curve of c_d vs Re in Fig. 8 can now be predicted. This curve is for the slot with the sharp entrance, for which $c_c c_v$ will be assumed to be 0.611 for turbulent flow. For example, at $Re = 7000$, using Eq. (2) with $f = 0.00682$, $K_v = 1$, and $c_c c_v = 0.611$, c_d is calculated to be 0.75, which is in excellent agreement with the experimental value of 0.74. Similarly, c_d can be predicted from Eq. (2) in the laminar region ($c_c c_v \cong 1.0$, $K_v = 1.6$).

D. Effect of Orifice Length on Discharge Coefficient

A more comprehensive indication of the effect of orifice length (nondimensionalized and expressed as the ratio L/t) on c_d is shown in Fig. 9 for a wide range of Reynolds numbers. At constant Re, c_d is maximized by minimizing L/t because of the contributions of fluid friction within the ducts.

A crossplot of selected data from Fig. 9 is presented in Fig. 10. Here it becomes more apparent that c_d is affected principally by L/t, with Re exerting a lesser effect which approaches second-order at high values of the Reynolds number; c_d extrapolates to 1.0 as $L/t \to 0$. This is reasonable, since the experiments were carried out in a regime ($L/t > 10$) where fully detached flow was not encountered. Had it been possible to conduct experiments at lower values of L/t ($0 \leqslant L/t \leqslant 10$), flow separation might have been encountered, and the limiting value of c_d (as $L/t \to 0$) would probably have approached a lower value.

The curves shown in Figs. 9 and 10 are not completely general; they apply strictly to orifices with a specific surface finish and entrance geometry. The effects of the major variables are believed to have been adequately demonstrated, however.

E. Hydraulic Flip

The phenomenon known as "hydraulic flip" (Ref. 7) was encountered with most orifices which had L/t ratios less than about 40. This was not surprising; short orifices of other cross sections, notably those that are circular, exhibit similar behavior. For the devices studied in the present investigation, the flip would have consisted of

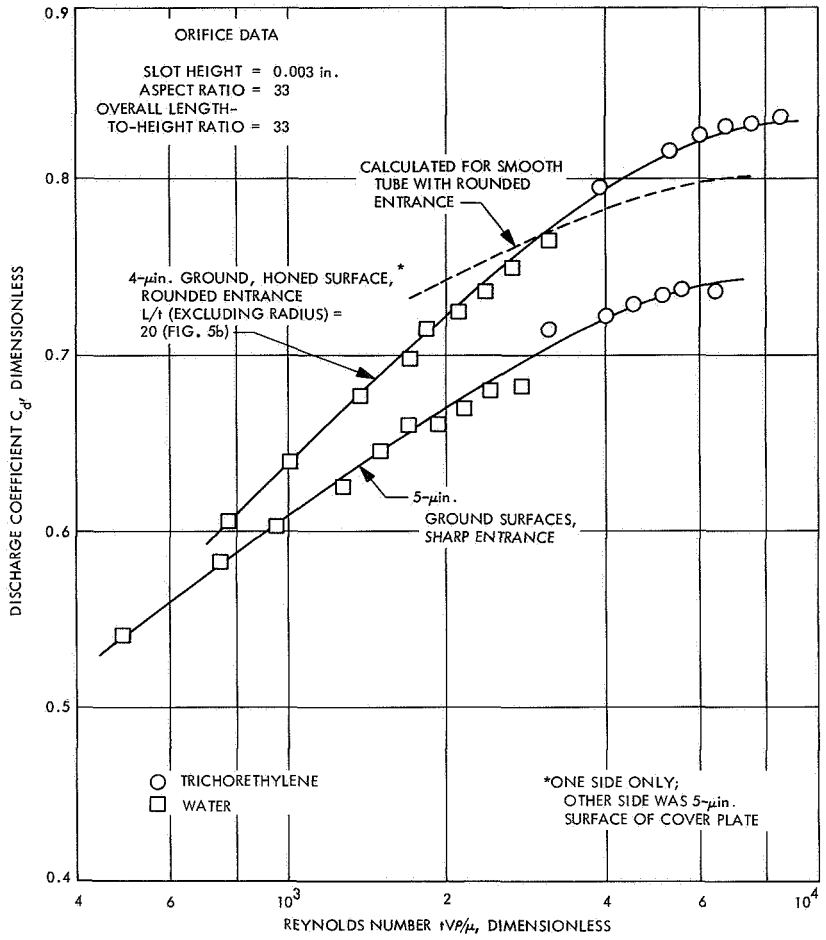

Fig. 8. Effect of orifice entrance on discharge coefficient for fixed geometry and surface finish

the sudden separation of the liquid stream from the surface S2 along its entire length L (see Fig. 2); the flow would have remained attached to the opposite wall S3. With attached flow on S3, there would have been little tendency for the flow to reattach to S2 at some point downstream of the separation point, so the symptoms of hydraulic flip were detected at L/t ratios as high as 40.

An example of this flip phenomenon is presented in Fig. 11 for water (a) and trichlorethylene (b). As the flow rate (expressed here as Re) is increased, a point is reached at which the flowing stream suddenly detaches itself from the wall S2 of the slot and flows free, with a correspondingly abrupt decrease in c_d. As the flow Re is decreased, the stream suddenly reattaches again, but at a lower value of Re than that encountered with increasing flow. This is the characteristic hysteresis loop associated with hydraulic flip. For simplicity, data points representing detached flow have been omitted from Figs. 9 and 10. As shown in Fig. 10, at $L/t = 40$, the highest values of c_d to be expected for hydraulically stable micro-orifices ($L/t \geqq 40$) with this particular kind of surface and entrance conditions range between 0.54 and 0.75, depending on Re. These low values of c_d imply that rather high pressure drops may be necessary to maintain a given level of flow. Lowering L/t to alleviate this situation may, however, lead to hydraulic instability.

Values of c_d just prior to hydraulic flip may be predicted by Eq. (2). Since the orifices from which the data of Fig. 11 were generated had sharp entrances, $c_c c_v$ may be assumed to be 0.611. The friction factor for a 5-μin. surface near $Re = 2000$ was shown earlier to be 0.0138, and is close to 0.01 near $Re = 3000$. As will be discussed in the following subsection of this report, the pre-flip flow through the orifices (Fig. 11) was *transitional*, and not completely turbulent. Accordingly, a reasonable intermediate value of K_v ($\sim$1.24) must be assumed. The use of these values in Eq. (2) enables prediction of the pre-flip c_d values for Fig. 11a and b to be 0.65 and 0.67, respectively, which are in excellent agreement with the experimentally determined values.

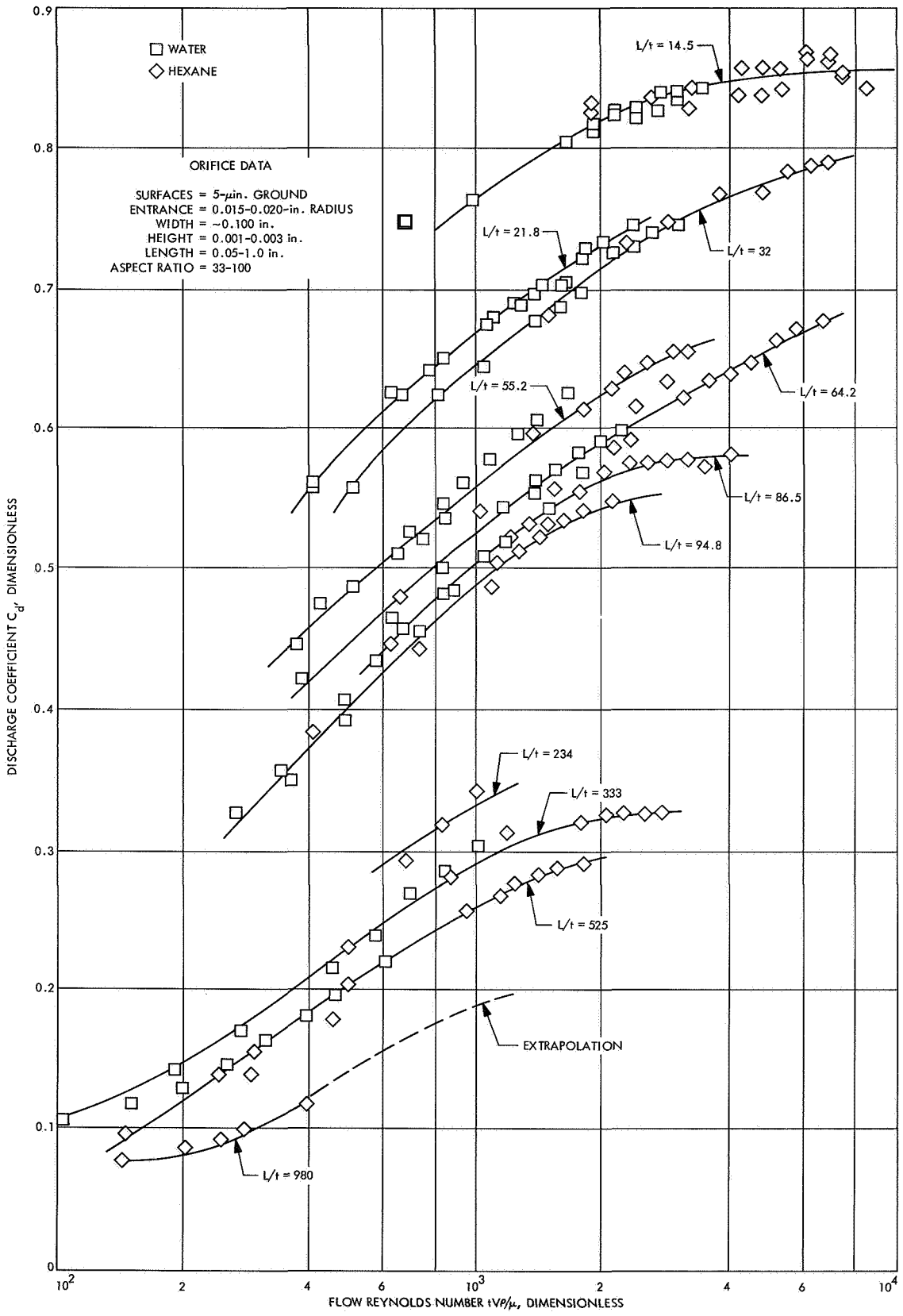

Fig. 9. Effect of orifice length on discharge coefficient

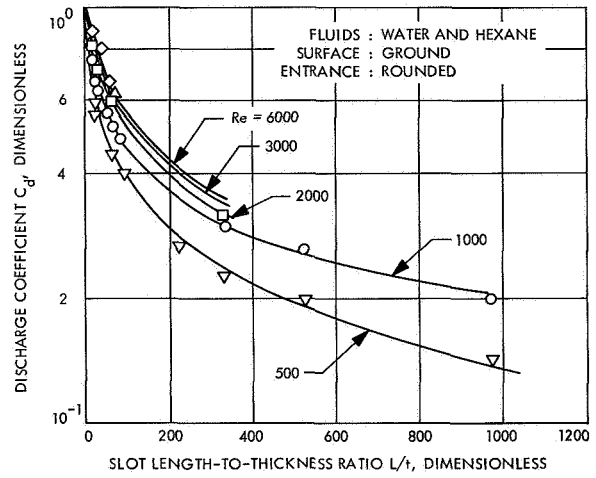

Fig. 10. Effect of slot geometry and Reynolds number on discharge coefficient

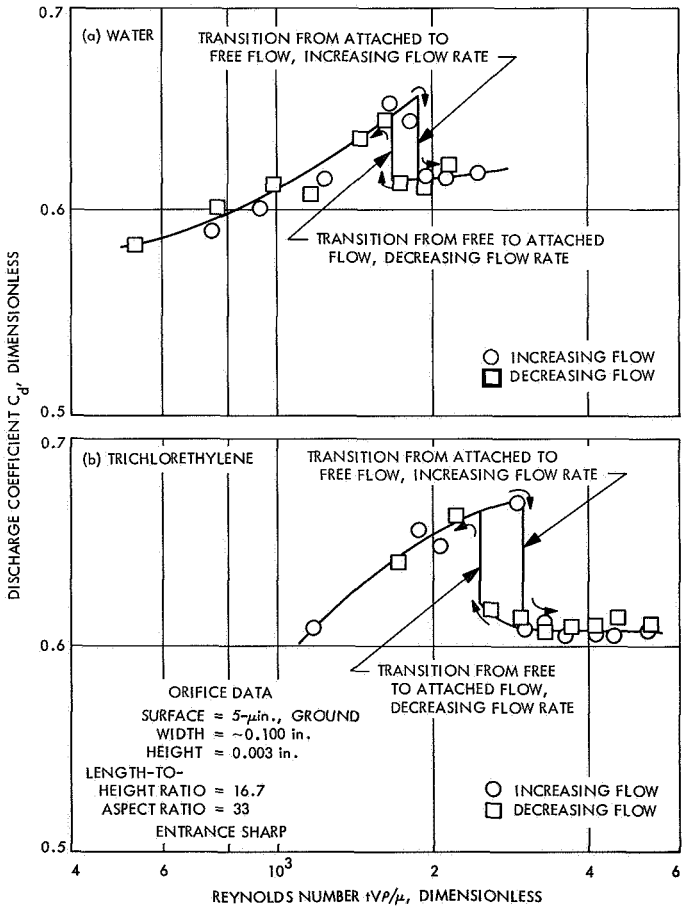

Fig. 11. Hydraulic flip of short orifice

The Reynolds number at which flip occurs may be estimated from Eq. (A-16) (see Appendix). Using the aforementioned values of $c_c c_v$, f, and K_v, in conjunction with the density, viscosity, and vapor pressure of water and trichlorethylene, enables one to predict that at atmospheric pressure, flip will occur at $Re = 1900$ for water and 3060 for trichlorethylene. Both of these values are in excellent agreement with the experimental results of Fig. 11. Similarly, the post-flip values of c_d of about 0.61 are in agreement with those predicted by Eq. (A-10) (see Appendix).

In the case of a firing rocket engine, "ambient" pressure equals chamber pressure, ($p_a = p_c$), and the Reynolds number at which hydraulic flip will occur is increased substantially. Thus, hydraulic flip may be encountered only at very high flow rates with orifices of this type under firing conditions.

F. Effects of Orifice Length and Reynolds Number on Flow Regime

The relationship between the mass flow rate through an orifice and the corresponding pressure differential across that orifice is of importance in injector throttling applications. If the flow through a very long slot is purely laminar, for example, the pressure drop is directly proportional to the mass flow rate. That is, the exponent b is unity in the relation

$$\Delta p \sim (\dot{w})^b \tag{8}$$

so a tenfold change in mass flow would require a tenfold change in pressure drop. On the other hand, if the flow in a very short orifice were in the region of Reynolds number similarity, the exponent b in Eq. (8) would be 2, and a hundredfold change in Δp would be required to effect the tenfold change in $\dot{w}$. In intermediate or transitional flow regimes, $1 < b < 2$. For throttling applications, then, the exponent b emerges as a parameter of great interest.

The gross nature of the measurements made during this study makes it difficult to authoritatively classify the various flows obtained as definitely "laminar," "turbulent," or "transitional." Velocity profiles, levels of turbulence, and the like, were not measured. Therefore, in the following discussion, the flows will be characterized mainly in terms of the empirical exponent b of the power-law relation of Eq. (8).

Values of the exponent b were determined by differentiating, both graphically and analytically, the curves of Δp vs $\dot{w}$ obtained for each of the flow devices. The results are plotted in Fig. 12, which shows how b varied with Reynolds number and orifice L/t ratio for ground slots with rounded entries.

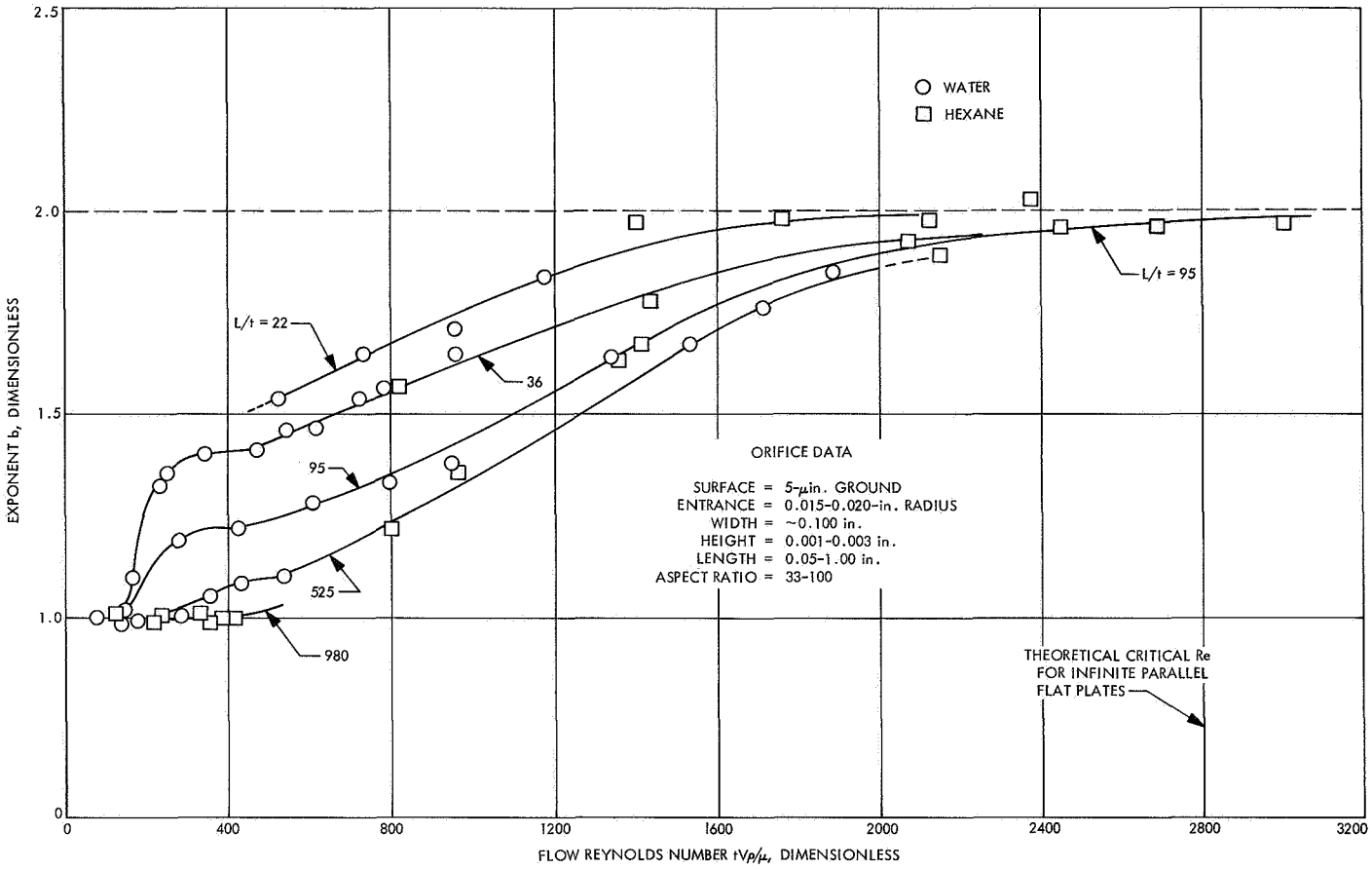

Fig. 12. Variation of exponent *b* with Reynolds number and orifice length

Examination of Fig. 12 yields the striking observation that over wide ranges of L/t and Re, the exponent b lies *between* 1 and 2. If b may be taken as an index of the flow regime, *transitional* flow may be said to dominate for small, slot-like orifices; clear-cut laminar or turbulent behavior is in evidence only at the extremes of the ranges of variables, although low values of L/t and high values of Re tend to increase b. As Re is increased, the curves for all values of L/t appear to approach $b = 2$ asymptotically, having essentially attained that limiting value in the vicinity of $Re = 2800$. This is as expected, since that is the theoretical critical Re for flow between infinite, parallel flat plates, a condition approximated by flow in high-aspect-ratio slots. As a rule of thumb, then, Reynolds numbers in excess of 2800 appear necessary to assure Reynolds number-similar flow behavior ($b = 2$). If the orifices are long (low c_d), excessively high pressure drops may be required to achieve this condition.

Laminar-like flow, if desired, appears feasible only at Reynolds numbers of 400 or below, depending on the particular value of L/t. However, it was observed in these experiments that the correspondingly low flow rates required to achieve $b = 1$ often led to a "weeping" or "dribbling" of effluent from the orifice, rather than discrete streams of liquid (Fig. 13a). In practical rocket engine injectors, where vigorous stream interactions are usually essential to promote propellant mixing and atomization, the resultant stream velocities may be too low. The designer may find, therefore, that linear propellant throttling and high combustion efficiencies are mutually incompatible.

In the dominant "transitional" ($1 < b < 2$) region, $b = f(Re)$ for any fixed value of L/t and will, therefore, change as the flow rate is varied during throttling. Accurate prediction of flow rates during such throttling is, therefore, predicated on detailed hydraulic data describing the behavior of individual slots of the type used in the injector, and cannot proceed *a priori* as it would for purely laminar or turbulent flow.

G. Visual Characteristics of Streams From Slot Orifices

A number of high-speed, microflash still photographs were taken of streams of water and hexane emerging

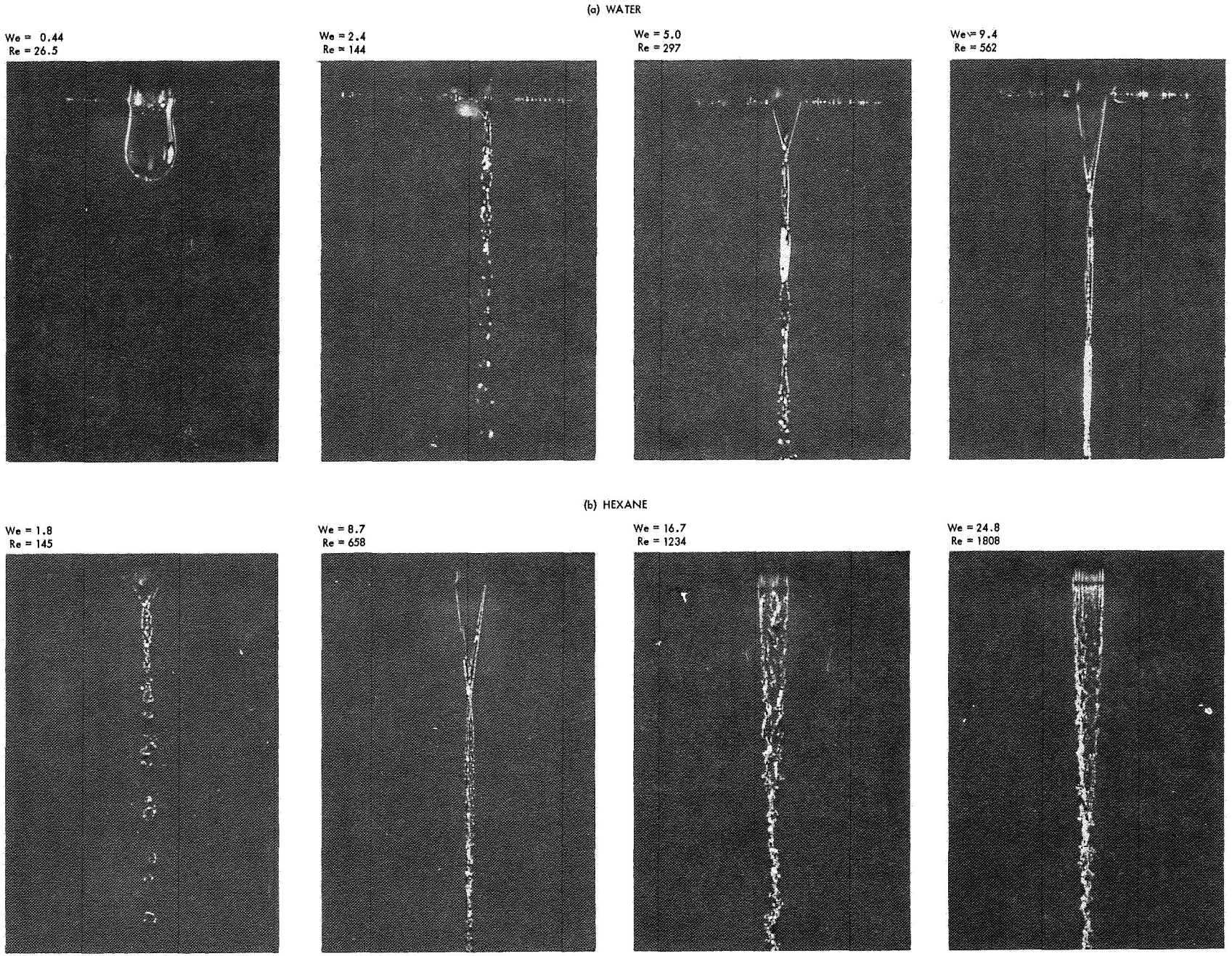

Fig. 13. Visual appearance of streams formed by 0.002-in. ground surface slot with two fluids (aspect ratio = 53.4; $L/t = 525$)

from the micro-orifice slots. A sampling of these photographs is presented in Fig. 13. The streams were characteristically flat sheets with the predominant edge ribs commonly observed in the flow from rectangular orifices (Ref. 8). They assumed a typically triangular shape. The apex angle was found to decrease with increasing flow rate and to increase with increasing liquid surface tension. This observation suggested that the apex angle was sensitive to the balance between inertial and surface forces on the sheet. Not surprisingly, then, a good correlation was found between the apex angle β and the ratio of these two forces, the Weber number. This is shown in Fig. 14. For the ranges $36 \leq L/t \leq 525$ and $2 < We < 30$, the two are related by

$$\beta \cong 135\, We^{-1} \tag{9}$$

It would be expected that β would depend on the orifice width w, as well as the height t. However, all the devices used in this study were of constant width (0.100 in.), so it was not possible to evaluate the extent of that effect. The width employed was typical of those used in slot-type rocket injectors, however, making the present results applicable to their design.

The number shown next to each data point in Fig. 14 is the corresponding value of the Reynolds number. In the overlap region between the two fluids ($8.5 < We < 9.2$) there is a wide variation in Reynolds number ($426 < Re < 658$), but good correlation in terms of Weber number alone is still possible. This is an indication of the Reynolds number independence of the sheet spreading angle.

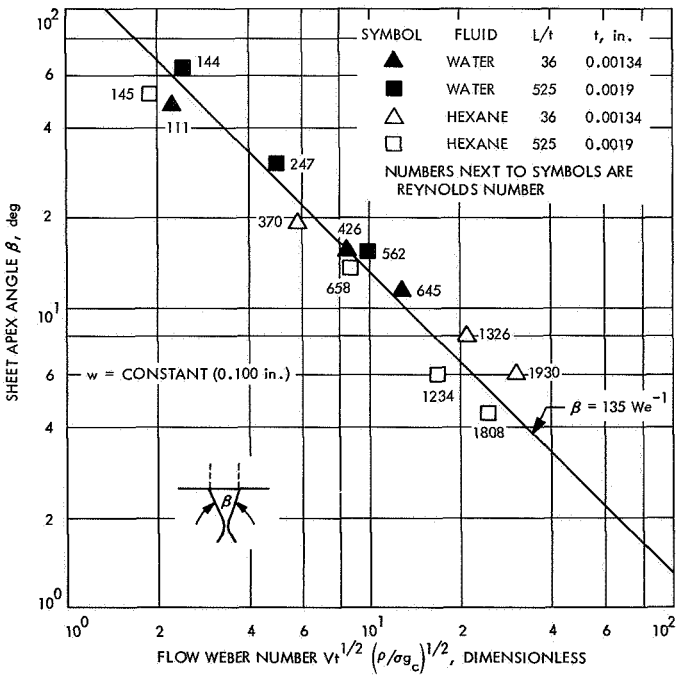

Fig. 14. Variation of sheet apex angle with flow Weber number

The effluent sheets also exhibited the surface tension phenomenon known as "inversion" (Ref. 9) characteristic of streams emerging from flat or elliptical orifices. That is, at regular distances downstream from the orifice, the sheet circularized, but then overshot and became elliptical, with its long axis at 90 deg to that of the original sheet in the plane of its cross section. These inversions were stable in time. This effect is shown in some of the low-flow-rate photographs in Fig. 13 (at high flow rates stream breakup occurred beyond the first node), and also in the side view of Fig. 15.

Unlike the jets produced by circular orifices, therefore, the sheets formed by such slots do not exhibit a constant cross-sectional area with axial distance. Thus, if the streams are intended to impinge at some point in space external to the orifices, their initially triangular geometry and successive inversions must be considered in laying out the relative positions of the slots.

H. Stability of Streams From Slot Orifices

The high-speed motion pictures taken of streams of water and hexane emerging from the rectangular slots revealed a remarkable stability in their dimensions and direction with respect to time. This was true for flow rates in the laminar, transitional, and turbulent regimes, and for L/t ratios ranging between 36 and 980. Figure 16 shows three successive frames from one of the films, taken at intervals of 2.5×10^{-4} s, which are typical of all the results obtained with regard to dimensional stability. The orifice of Fig. 16 was only 0.1 in. long.

These results may be contrasted to those of Ref. 10, where similar cinematography showed the jets emerging from short square-edged orifices of circular cross section to be inherently unstable, writhing and flickering about at random. High values of orifice length do not appear to be as necessary to assure stable streams with miniature rectangular slots as they are with conventional round jets.

I. Practical Limitations on Slot Depth

For the most part, the streams formed from the thinnest slots ($t \cong 0.001$ in.) were degraded to various extents at high flow rates and would probably be unsuitable for use in a rocket engine injector. As shown in

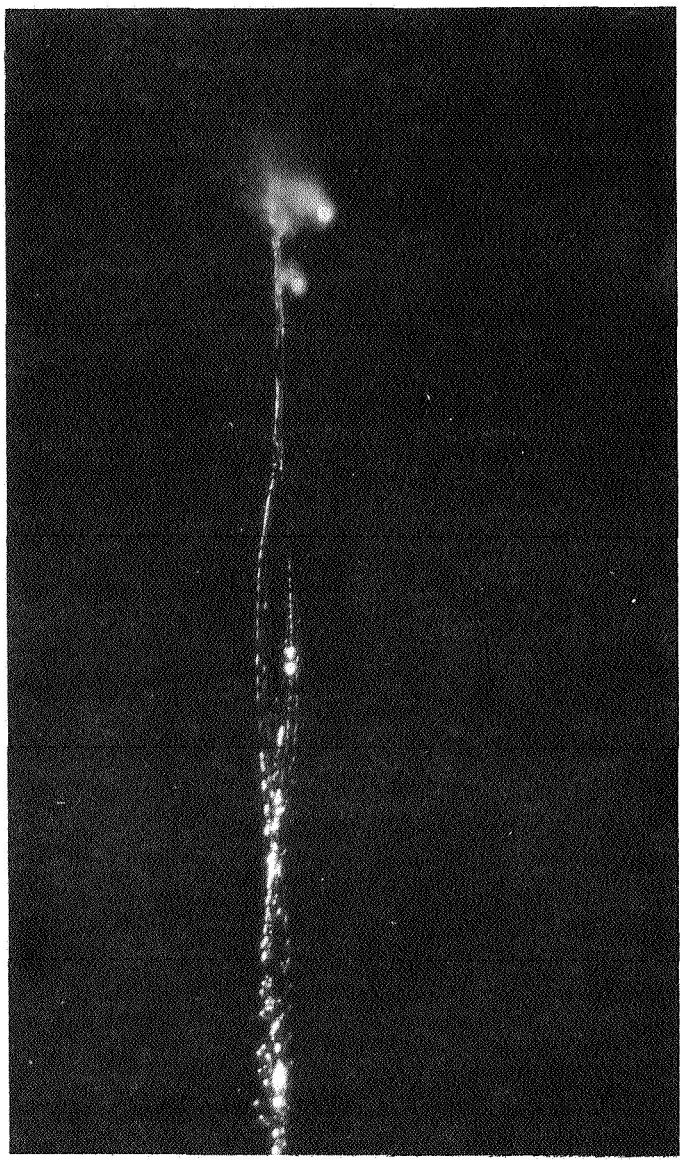

Fig. 15. Side view of hexane stream from high-aspect-ratio slot showing characteristic inversions (0.002 × 0.100-in. slot)

Fig. 17, for example, striated flows consisting mainly of individual filaments were formed in preference to planar sheets. Stream disintegration was enhanced under these conditions. This effect is probably due to the fact that the dimension of the surface finish marks becomes large enough relative to the slot height to influence the flow for very thin slots. In addition, clogging of the orifices by foreign particulate matter proved to be a major operational problem for the 0.001-in. slots. A slot height of 0.002 in., at which neither of the foregoing problems was encountered, would, therefore, be recommended as the minimum practical value of this dimension.

V. Summary of Results

The experimental results may be summarized as follows:

A. Effect of Surface Finish on Discharge Coefficient

The discharge coefficient was found to be sensitive to both the surface finish of the interior of the rectangular duct, and to its entrance geometry. This value could be increased, resulting in a greater mass flow through the orifice for a given pressure differential across it, by using smoother surface finishes and rounded entries. Since the surface finish is, in turn, related to the process by which the orifices are formed (grinding, stamping, electric-discharge or chemical machining, etc.), the hydraulic characteristics of this type of orifice would be expected to be strongly influenced by fabrication techniques.

B. Effects of Orifice Length and Reynolds Number on Discharge Coefficient

For a given orifice cross-section, surface finish, and entrance configuration, the discharge coefficient depends mainly on the ratio L/t of length to height, and is affected to a lesser degree by the Reynolds number. Low values of L/t and high Reynolds numbers tend to maximize the discharge coefficient.

C. Hydraulic Flip

Hydraulic flip, a form of flow instability, was encountered when the L/t ratio was less than about 40. The data indicated that the highest values of c_d for hydraulically stable orifices ranged between 0.54 and 0.75 (depending on Re) for the particular surface finishes and entrance conditions tested. These low values of c_d imply that rather high values of pressure drop may be required to maintain a given level of flow.

D. Visual Characteristics of Streams From Slot Orifices

Over a wide range of operating conditions, the orifices studied exhibited flow that was transitional, rather than purely laminar or turbulent. That is, $1 < b < 2$ in the relation, $\Delta p \sim \dot{w}^b$. Reynolds numbers in excess of 2800 were found necessary to assure turbulent flow, whereas exceedingly low Reynolds numbers (< 400) and long orificies were required for laminar flow. Thus, for most throttling applications, the relationship between mass flow rate and pressure drop would be expected to be a somewhat involved function of Re and L/t.

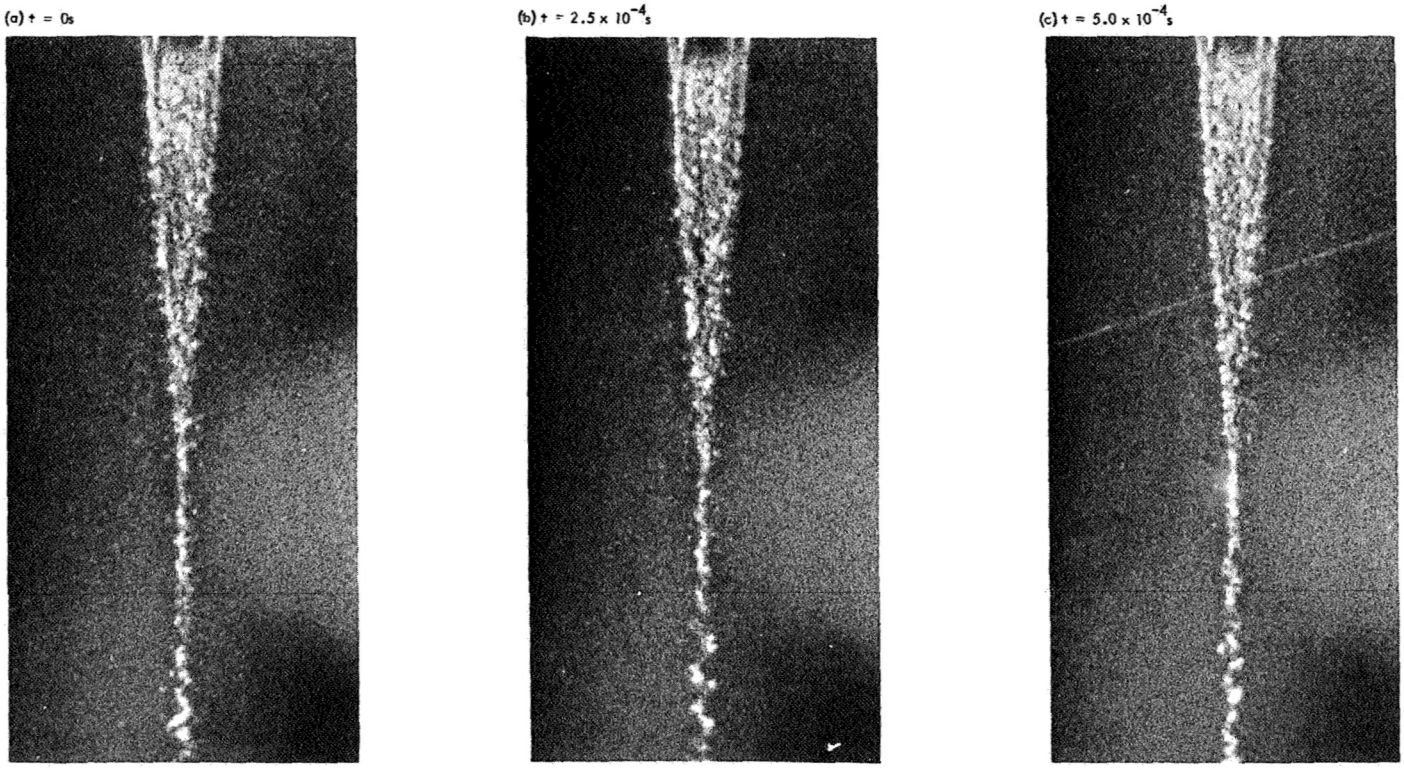

Fig. 16. Example of stability of sheet from short slot orifice (0.001 × 0.100-in. slot)

E. Stability of Streams From Slot Orifices

The streams emerging from the slot-like orifices were found to be highly stable, planar, and initially triangular in shape. The apex angle of the triangle was shown to vary inversely with the Weber number, and the streams exhibited the inversions typical of sheets formed from rectangular or elliptical orifices. This unconventional stream behavior (compared to jets issuing from round orifices) suggests that greater care be taken in the design of micro-orifice injectors, especially those involving stream impingement, than is usual for the common jet varieties.

F. Practical Limitations on Slot Depth

A minimum slot height of 0.002 in. is recommended to avoid orifice clogging and stream degradation.

VI. Concluding Remarks

The hydraulic characteristics of liquid flow through miniature rectangular orifices of high aspect ratio have been studied quantitatively, although not in great depth. The results were, for the most part, not surprising; the general effects of the principal variables were similar to those already well known for the flow of liquids through ordinary round holes.

Manufacturers and users of injectors with such orifices should be interested, however, in the observations regarding the effects of surface finish (and, therefore, manufacturing processes) on flow characteristics, the relatively unusual shape and behavior of the free streams, and the predominantly transitional nature of the flow.

Roughness, in particular, exerts a major influence on orifice discharge, and must be carefully controlled.

While by no means complete, the quantitative information developed in this study is directly applicable to the design of liquid-propellant rocket engine injectors of the so-called micro-orifice class.

(a) HEXANE, Re = 2800

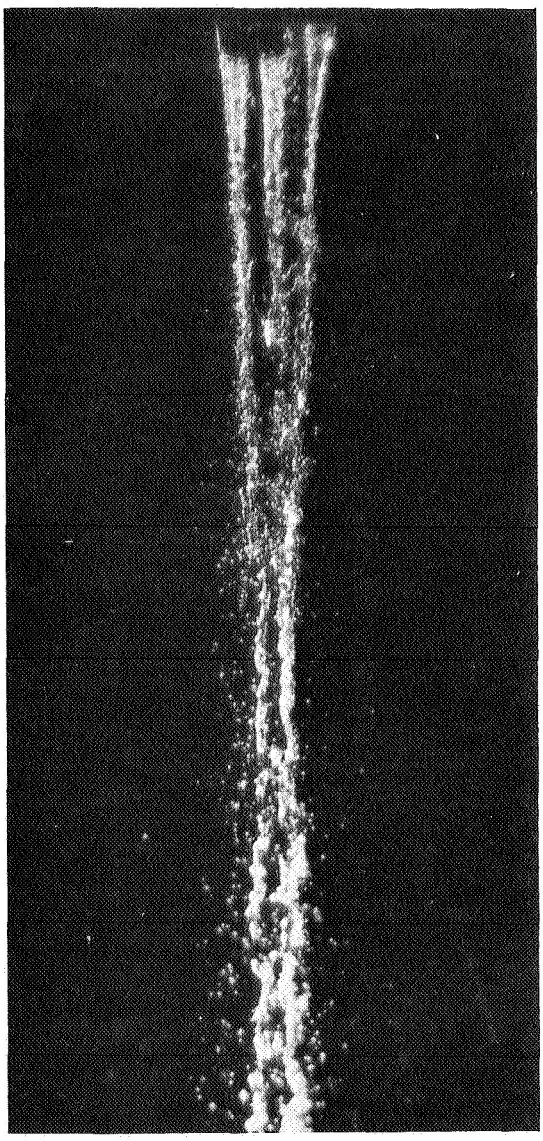

(b) WATER, Re = 1040

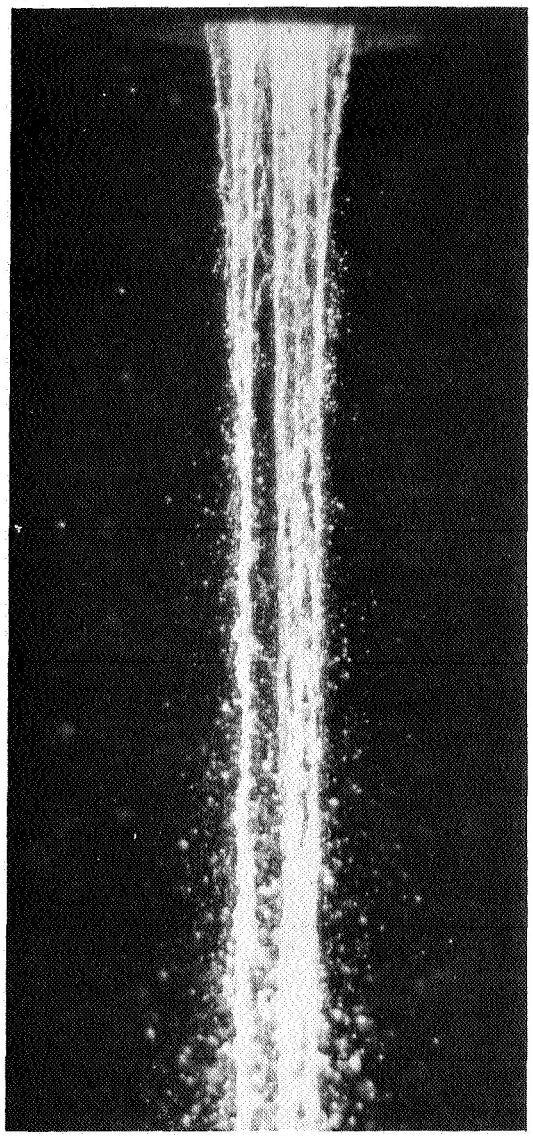

Fig. 17. Degradation of streams from short, thin slots at high Reynolds numbers ($t = 0.001$ in.; $L/t = 35.8$)

Appendix

Orifice Flow Model

Consider an orifice of arbitrary sectional area A_j, fed by a liquid of density ρ and viscosity μ from an infinitely large reservoir, as in Fig. A-1. The liquid mass flux throughput $\dot{w}$ enters at velocity $V_o \cong 0$ and leaves at $\bar{V}_j$. Assume the liquid contracts upon entering, forming a vena contracta of area A_t at which the pressure and velocity are p_t and $\bar{V}_t$, respectively, then expands turbulently, conserving its momentum, reattaches to the conduit walls, and flows full for the length L before exiting the orifice. Assume further that friction acts only over the length L. The pressure drop between the entrance and the vena contracta may be written as:

$$p_o - p_t = \frac{\rho \bar{V}_j^2}{2g_c c_c^2 c_v^2} \tag{A-1}$$

where $c_c \equiv A_t/A_j$ and c_v is the ratio of the actual throat velocity V_t to the throat velocity corresponding to isentropic contraction. Since the net force acting on the fluid must equal the net momentum flux, the pressure change between the vena contracta and the exit is

$$p_t A - p_a A - \frac{\rho \bar{V}_j^2 f A_s}{2g_c} = \frac{K_v \dot{w} \bar{V}_j}{g_c} - \frac{\dot{w} \bar{V}_j}{c_v c_c g_c} \tag{A-2}$$

where A_s is the duct surface area, corresponding to the length L, over which the friction force acts, f is the Fanning friction factor, and K_v is a momentum increment factor which reflects variations in the velocity profile; $K_v = 1$ for turbulent flow, 1.6 for laminar flow, and exhibits intermediate values in the transition region. Upon incorporating the continuity principle, Eq. (A-2) may be simplified to

$$p_a - p_t = \frac{\rho \bar{V}_j^2}{2g_c}\left[\frac{2}{c_c c_v} - 2K_v - f\left(\frac{A_s}{A}\right)\right] \tag{A-3}$$

The net pressure drop between stations o and a may then be found by summing Eqs. (A-1) and (A-3):

$$p_o - p_a = \frac{\rho \bar{V}_j^2}{2g_c}\left[\frac{1}{c_v^2 c_c^2} + 2K_v - \frac{2}{c_c c_v} + f\frac{A_s}{A}\right] \tag{A-4}$$

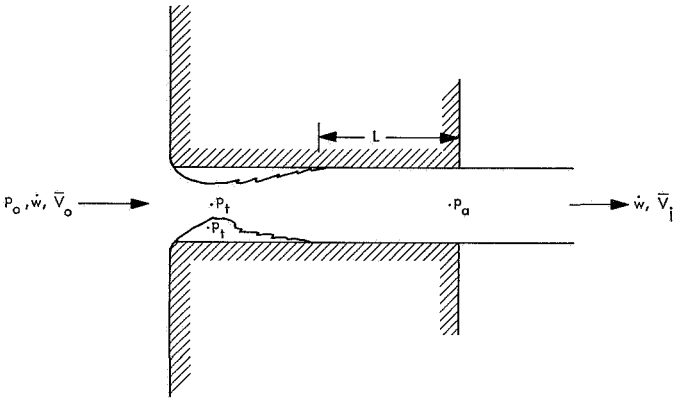

Fig. A-1. Schematic representation of generalized orifice

Since the discharge coefficient c_d is defined as

$$c_d = \left[\frac{\rho \bar{V}_j^2}{2g_c(p_o - p_a)}\right]^{1/2} \tag{A-5}$$

combination of Eqs. (A-4) and (A-5) yields

$$c_d = \left[\frac{1}{c_v^2 c_c^2} + 2K_v - \frac{2}{c_c c_v} + f\left(\frac{A_s}{A}\right)\right]^{-1/2} \tag{A-6}$$

As the flow through the orifice is increased, p_t will decrease. If it decreases until it equals the vapor pressure of the liquid, p_v, cavitation will occur in the separated region, generating large quantities of vapor which seek an exit. Expansion and reattachment then cease, and the jet flows free of the walls; $p_t = p_a$ because of the access of the separated region to the downstream region. Hydraulic flip is then said to have occurred.

The "critical velocity" of the jet just before flip occurs, when $p_t = p_v$, may be found from Eq. (A-3) to be

$$\bar{V}_{crit} = \frac{(p_a - p_t)^{1/2}(2g_c)^{1/2}}{\rho^{1/2}\left[\frac{2}{c_c c_v} - 2K_v - f\left(\frac{A_s}{A}\right)\right]^{1/2}} \tag{A-7}$$

Incorporation of the definition of Reynolds number

$$Re = \frac{t\bar{V}\rho}{\mu} \tag{A-8}$$

gives

$$Re_{crit} = \frac{\rho^{1/2} t\,(p_a - p_v)^{1/2}\,(2g_c)^{1/2}}{\mu\left[\dfrac{2}{c_c c_v} - 2K_v - f\left(\dfrac{A_s}{A}\right)\right]^{1/2}} \tag{A-9}$$

as the critical Reynolds number at which hydraulic flip will occur as flow is increased.

After flip has occurred, the jet may remain separated from the walls, and with no friction, expansion or reattachment losses,

$$c_d \cong c_c c_v \tag{A-10}$$

Thus, the discharge coefficient just prior to flip may be predicted by Eq. (A-6), that immediately after flip by Eq. (A-10), and the Reynolds number at the flip point by Eq. (A-9). If the duct is sufficiently long, reattachment and reabsorption of vapor bubbles may occur, in which case Eq. (A-6) would apply at all times.

The situation for the slots studied in this report is represented by Fig. A-2. Here, separation occurs along one side only. For a rectangular slot,

$$A_s = 2L(w + t) \tag{A-11}$$

and

$$A = wt \tag{A-12}$$

Thus,

$$\frac{A_s}{A} = \frac{2L(w + t)}{wt} \tag{A-13}$$

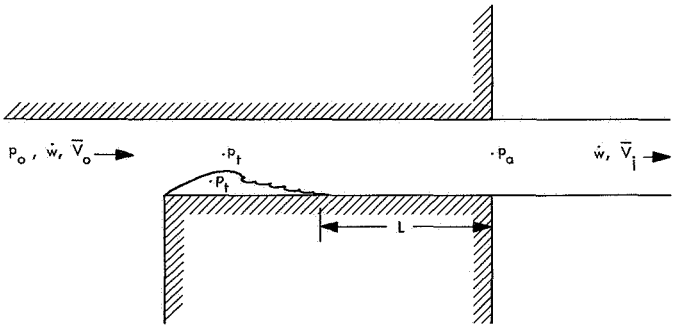

Fig. A-2. Schematic representation of slot orifice from present study

But since $w \gg t$,

$$\frac{A_s}{A} \cong \frac{2L}{t} \tag{A-14}$$

Then the discharge coefficient prior to flip is given by

$$c_d = \left(\frac{1}{c_v^2\, c_c^2} + 2K_v - \frac{2}{c_c c_v} + \frac{2fL}{t}\right)^{-1/2} \tag{A-15}$$

and the Reynolds number at incipient flip is

$$Re_{crit} = \frac{\rho^{1/2} t\,(p_a - p_v)^{1/2}\,(2g_c)^{1/2}}{\mu\left(\dfrac{2}{c_c c_v} - 2K_v - \dfrac{2fL}{t}\right)^{1/2}} \tag{A-16}$$

As before, the discharge coefficient after flip is $c_c c_v$ if reattachment does not occur.

The theoretical value of the contraction coefficient for turbulent flow through a sharp-edged slot of high aspect ratio, in which flow separation occurs on both sides, is

$$c_c \equiv \frac{\pi}{\pi + 2} = 0.611 \tag{A-17}$$

By symmetry, the theoretical c_c for the slots used in the present experiments, where separation occurs on one side only, is also given by Eq. (A-17). Smith and Walker (Ref. 11) report actual values of c_c for circular, sharp-edged orifices, which vary between 0.613 for large (2.5 in.) diameters at high flow rates and 0.688 for small (0.75 in.) diameters at low flow rates. By analogy with this circular orifice data, one would expect a similar range of values for slot-orifice contraction coefficients.

The same authors report an opposite variation in actual values of c_v measured for circular, sharp-edged orifices. That is, $c_v = 0.993$ for the large diameters and high flow rates, whereas $c_v = 0.954$ for the small diameters and low flow rates. Thus, for circular sharp-edged orifices there is less variation in the product $c_c c_v$ than in its individual components, and the same may be supposed to be true for sharp-edged slots. Thus, the product $c_c c_v$ may be expected to vary between 0.61 and 0.66, increasing as slot height decreases, and may be even greater for slots with dimensions as small as those employed in the present study. In laminar flow, separation does not occur, and $c_c c_v \cong 1.0$.

As already pointed out, K_v has limiting values of 1.0 and 1.6 for turbulent and laminar flow, respectively. However, since many of the slots investigated in this study exhibited transitional flow, less-well-defined values of K_v, ranging between these two extremes, may be expected.

The standard Fanning friction factor chart may be used to determine values of f, except that the chart must be entered at values of Re equal to twice those used in this report because of differences in the definition of the hydraulic diameter.

For surface finishes of 5 μin. rms, the smooth-tube curves may be used, as demonstrated by the dashed curve of Fig. 8. The friction factor may be expected to range between about 0.008 and 0.02.

Nomenclature

A	orifice area, in.^{2}
c_c	contraction coefficient, dimensionless
c_d	orifice flow index, dimensionless
D_h	hydraulic diameter, in.
f	Fanning friction factor, dimensionless
g_c	gravitational constant, 32.174 (lbm-ft)/(lbf-sec^2)
K_v	momentum increment factor, dimensionless
L	orifice length, in.
p_a	ambient pressure, psia
p_c	chamber pressure, psia
p_v	vapor pressure, psia
Re	Reynolds number, dimensionless
t	slot height, in.
$\bar{V}$	average fluid velocity, ft/s
w	slot width, in.
$\dot{w}$	mass flow rate, lb/s
We	Weber number, dimensionless
β	sheet apex angle, deg
μ	liquid viscosity, lb/ft-s
ρ	liquid density, lb/ft^3
σ	liquid surface tension, lb/ft

Subscripts

crit	critical
j	jet
o	entrance
s	duct surface
t	throat
v	velocity

References

1. McGough, C. B., La Botz, R. J., and Addoms, J. F., "Development of HIPERTHIN Injectors for Reaction Control Thruster Application," paper presented at ASME 1968 Aviation and Space Conference, Los Angeles, Calif., June 1968.

2. Adelberg, M., and Arnold, M. M., "Micro-Orifice Injectors and Combined Injector/Chambers for Improved Liquid Rocket Motor Design Concepts," paper presented at Eighth Liquid Propulsion Symposium (CPIA), Cleveland, Ohio, Nov. 1966.

3. Heckert, B. J., *Experimental Wound Ribbon Injector Evaluation,* Report MR 20,390A. Astro, The Marquardt Corporation, Van Nuys, Calif., Mar. 1967.

4. Sparrow, E. M., and Haji-Sheikh, A., "Flow and Heat Transfer in Ducts of Arbitrary Shape With Arbitrary Thermal Boundary Conditions," *J. Heat Transfer,* Vol. 82, No. 4, Section C, p. 351, Nov. 1966.

5. Hanks, R. W., and Ruo, H. C., "Laminar-Turbulent Transition in Ducts of Rectangular Cross-Section," *I&EC Fundamentals,* Vol. 5, No. 1, p. 558, Feb. 1966.

6. Hanks, R. W., and Song, D. S., "Experimental Investigation of the Laminar-Turbulent Transition for Newtonian Flow in Rectangular Ducts," *I&EC Fundamentals,* Vol. 6, No. 3, p. 472, Aug. 1967.

7. Northup, R. P., "Flow Instability in Small Orifices," Paper ARS 49-51, presented at ASME Meeting, Atlantic City, N. J., Nov. 30, 1951.

8. Dombrowski, N., and Fraser, R. P., "A Photographic Investigation into the Disintegration of Liquid Sheets," *Phil. Trans. Roy. Soc. London, Ser. A,* Vol. 247, p. 101, 1954.

9. Taylor, G., "Formation of Thin Flat Sheets of Water," *Proc. Roy. Soc. London, Ser. A,* Vol. 259, p. 1, 1960.

10. Riebling, R. W., *The Formation and Properties of Liquid Sheets Suitable for Use in Rocket Engine Injectors,* Technical Report 32-1112. Jet Propulsion Laboratory, Pasadena, Calif., June 15, 1967.

11. Smith, D., and Walker, W. J., "Orifice Flow," *Proc. Inst. Mech. Eng.,* (London), p. 23, 1923.